Anucleated cryptophyte endosymbionts in the gonyaulacalean dinoflagellates, *Amylax buxus* and *Amylax triacantha* (Dinophyceae)

Kazuhiko Koike[1*] and Kiyotaka Takishita[2]

[1] Graduate school of Biosphere Science, Hiroshima University. Kagamiyama, Higashi-Hiroshima, Hiroshima 739-8528, Japan.

[2] Extremobiosphere Research Center, Research Program for Marine Biology and Ecology, Japan Agency for Marine-Earth Science and Technology. Natsushima, Yokosuka, Kanagawa, 237-0061, Japan.

*To whom correspondence should be addressed
Graduate school of Biosphere Science, Hiroshima University. Kagamiyama, Higashi-Hiroshima, Hiroshima 739-8528, Japan.
TEL: 81 82 424 7996, FAX: 81 82 424 7916, e-mail: kazkoike@hiroshima-u.ac.jp

Running title: Cryptophyte endosymbionts in *Amylax*

SUMMARY

Cryptophyte endosymbionts, suffering selective digestion of nuclei, were found in gonyaulacalean dinoflagellates, *Amylax buxus* (Balech) Dodge and *Amylax triacantha* (Jörgensen) Sournia. They emitted bright yellow-orange fluorescence (= 590 nm emission) under epifluorescent microscopy and possessed U-shape plastids. Under transmission electron microscopy, the plastid was characterized with loose arrangement of two to three thylakoids stacks and with stalked pyrenoid, all coincide to those of cryptophyte genus *Teleaulax*. Indeed, molecular data based on plastid small subunit rRNA gene demonstrated that the endosymbionts in *Amylax* are originated from *Teleaulax amphioxeia*. The stolen plastid (kleptoplastids) in *Dinophysis* is also acquired from this cryptophyte species. However, in sharp contrast to the case of *Dinophysis*, the plastid of endosymbiont in *Amylax* was surrounded by double layer of plastid endoplasmic reticulum, and within the periplastidal area, nucleomorph was retained. The endosymbionts also possessed mitochondria with characteristic plate-like cristae, but lost cell-surface structure. Dinoflagellate's phagocytotic membrane seemed to surround the endosymbionts right after the incorporation, but the membrane itself would probably be digested eventually. Remarkedly, only one cryptophyte cell among 14 endosymbionts in a cell of *A. buxus* had a nucleus. This is a first finding of kleptoplastidy in gonyaulacalean dinoflagellates, and provides unique strategy of a dinoflagellate in which it selectively eliminate the endosymbiont nucleus.

Key words

Amylax, cryptophyte, dinoflagellate, endosymbiosis, kleptoplastidy, *Teleaulax*

INTRODUCTION

The vast majority of photosynthetic dinoflagellates possess a “peridinin-type” plastid, that is pigmented by peculiar carotenoid, peridinin, while a few but phylogenetically diverged species contain plastids in which pigmentation patterns are different from the peridinin-containing plastids. Such “non-canonical” dinoflagellate plastids are similar to those of other eukaryotic algae in pigment composition and/or ultrastructural characterictics, implying that these types of plastids are remnants of endosymbiotic algae; e.g. chlorophyte (*Lepidodinium chlorophorum* (Elbrächter et Schnepf) Hansen *et al* and *Lepidodinium viride* Watanabe *et al*), haptophyte (genus *Karenia* Hansen et Moestrup, *Karlodinium* Lasen and *Takayama* De salas *et al.*), diatom (*Durinskia baltica* (Levander) Carty et Cox, *Kryptoperidinium foliaceum* (Stein) Lindemann (= *Glenodinium foliaceum* Stein), *Peridinium quinquecorne* Abe, *Gymnodinium quadrilobatum* Horiguchi et Pienaar, *Dinothrix paradoxa* Pascher). Some dinoflagellate species are actually skillful in acquiring foreign plastid, not only during the ancient evolutionary event but also in the present state. *Amphidinium poecilochroum* Lasen (Lasen, 1988), *Amphidinium latum* Lebour (Horiguchi & Piennar, 1992), *Gymnodinium aeruginosum* Stein (Schnepf *et al.*, 1989) (equivalent to *Gymnodinium* (*Amphidinium* ?) *acidotum* Nygaard in Wilcox & Wedemayer, 1985), *Gymnodinium gracilentum* Campbell (Skovgaard, 1998, Jakobsen *et al.*, 2000), *Cryptoperidiniopsis* sp. (Eriksen *et al.*, 2002), *Pfiesteria piscicida* Steidinger et Burkholder (Lewitus *et al.*, 1999) and photosynthetic *Dinophysis* spp. (Takishita *et al.*, 2002, Minnhagen & Janson, 2006) all they rob plastids from cryptophyte prey, and *Dinophysis mitra* (Shütt) Abe vel Balech (Koike *et al.*, 2005) and a *Karenia/Karlodinium* like dinoflagellate (Gast *et al.*,

2007) from haptophyte prey. These cases of transiently acquiring foreign plastids in environment are usually termed as kleptoplastidy. It remains uncertain that the stolen plastids are integrated into the host dinoflagellates at the genetic level, but such kleptoplastidy may imply an early stage of plastid endosymbiosis.

Because the dinoflagellate order Gonyaulacales Taylor is constantly monophyletic in the phylogeny (Saldarriaga *et al.*, 2004), it seems to be well-established order among dinoflagellates. It is mostly occupied with peridinin-containing species and no kleptoplastidic ones have been known among this order. If some typical gonyaulacalean species does undergoing of kleptoplastidy, then, this would much more emphasize evolutional flexibility in the plastid acquisition of dinoflagellates

Here, we show first evidence of cryptophycean kleptoplastid in gonyaulacalean species, *Amylax buxus* (Balech) Dodge and *Amylax triacantha* (Jörgensen) Sournia, and report here a unperceived way of “selective digestion of symbiont nucleus”.

MATERIALS AND METHODS

Collection of the cells and light microscopy

In the live plankton materials collected by vertical hauling of a 20 µm plankton net (from 20 m depth to the surface) in Okkirai Bay, Iwate, Japan (39° 05’ N, 141° 51’ E) on 30 May 2006, *Amylax* cells emitting orange fluorescence were observed under blue light excitation (emission 460 to 490 nm, barrier 515 nm) of an inverted epifluorescent microscope (IX71, Olympus, Tokyo, Japan). Light and fluorescent photomicrographs were taken using a 600 CL cooled digital camera

(Penguin, Los Gatos, CA, USA) connected to the inverted microscope. For species identification, the cells isolated by a capillary pipette were stained with calcofluor- white M2R (Sigma, St. Louis, MO, USA) as according to Fritz & Triemer, 1985, and the thecal plate tabulations were then observed under BX51 fluorescent microscope (Olympus).

In vivo *fluorescence spectrum.*

To confirm the *Amlylax* cells containing cryptophyte accessory pigment, phycobilin, *in vivo* fluorescent spectrum (400- 800 nm) under blue light excitation (emission 460 to 490 nm, barrier 515 nm) was measured in individual cells (n=10) using a photonic multi-channel analyzer (C7473, Hamamatsu Photonics, Shizuoka, Japan) attached to IX71 inverted fluorescence microscope.

Ultrastructure

Since two *Amylax* species (*A. buxus* and *A. triacantha*) coexisted in the sample, both species cells were separately isolated by capillary pipette and subjected to the preparation for the transmission electron microscopy (TEM), as according to our previous report (Koike *et al*., 2005). Ultrathin sections of each cell were cut with an Ultracut UCT ultratome (Leica Microsystems, Wetzlar, Germany) using a diamond knife. Sections were stained with saturated uranyl acetate in 50 % ethanol for 30 min and lead citrate for 3 min. Observations were made with a JEM-1011 transmission electron microscope (JEOL, Tokyo, Japan) operated at 80 kV.

PCR, cloning and sequencing

Cells of *A. buxus* and *A. triacantha* were separately isolated by capillary pipette and each 10 cells were transferred to 20 µL H_2O in a PCR tube. Two tubes were prepared for each species for; nuclear and plastid small-subunit (SSU) rRNA genes. Nuclear and plastid SSU rRNA genes were amplified by PCR with HotStarTaq (QIAGEN). The PCR primer sets for the amplification of nuclear and plastid SSU rRNA genes were 18S-42F+18S-1520R (Lopez-Garcia *et al.*, 2003) and PL16S1+PL16S2 (Takishita *et al.*, 1999), respectively. The thermal cycle conditions consisted of 35 cycles of 1 min at 94 ºC, 1 min at 50 ºC and 2 min at 72 ºC. The amplified DNA fragments of nuclear and plastid SSU rRNA genes were cloned into pCR2.1 TOPO TA vector (Invitrogen), and then sequenced with an ABI PRISM 3100 Genetic Analyzer (PE Biosystems) using a BigDye Terminator Cycle Sequencing Ready Reaction Kit (PE Biosystems). The sequences determine in this study were deposited under GenBank/EMBL/DDBJ accession numbers AB375868 - AB375871.

Phylogenetic analyses

Nuclear SSU rRNA gene sequence from the *Amylax* species determined in this study was aligned with the homologous sequences from 44 broadly sampled dinoflagellates and two apicomplexans by ClustalW (Thompson *et al.*, 1994). In addition, the *Amylax* plastid SSU rRNA gene sequences were aligned with the homologous sequences from 11 broadly sampled cryptophytes, 2 red algae and 4 species of the dinoflagellate genus *Dinophysis* by ClustalW. All ambiguously aligned sites were excluded from the phylogenetic analyses. The edited alignments (47 taxa/1674 sites of nuclear SSU rRNA gene and 19 taxa/1225 sites of plastid SSU rRNA gene) are available on request from the corresponding

author. For both alignments, Maximum-likelihood (ML) and Bayesian analyses were conducted. ML analyses were performed using PhyML (Guindon & Gascuel, 2003) using an input tree generated by BIONJ with general-time-reversible models (Rodríguez *et al.*, 1990) of nucleotide substitution incorporating invariable sites and a discrete gamma distribution (eight categories) (GTR + I + Γ model). Model parameters were estimated from the dataset. ML bootstrap trees (200 replicates) were constructed as in the model and settings described above. Bayesian phylogenetic analyses were conducted using MrBayes version 3.0 (Ronquist & Huelsenbeck, 2003) under GTR + I + Γ models. One cold and three heated Markov chain Monte Carlo (MCMC) chains with default-chain temperatures were run for 2,500,000 generations, sampling log-likelihoods (InLs) and trees at 100-generation intervals (25,000 InLs and trees were saved during MCMC). The likelihood plot for all datasets suggested that MCMC reached the stationary phase after the first 5,000 trees (i.e., the first 500,000 generations were set as “burn-in”). Thus, clade probabilities and branch-length estimates were obtained from the remaining 20,000 trees.

RESULTS

Light microscopy and species identification

The *Amylax* cells occurred at very low density (at most 1 - 5 cells mL^{-1} in 1 L of the plankton-net sample) in the field. The occurrences were barely able to be detected during 11 – 30 May 2006. The cells were recognized as a genus *Amylax* Meunier due to its apical long horn and antapical spines, and the two types of cells, one with somewhat rounded hypotheca and more brownish color

(Fig. 1a), and the other with the epitheca concaving leading to the long tapering apical horn and more distinctive antapical spine (Fig. 1c), were distinguished. Together with these cellular outlines and the thecal tabulation patterns, mostly to existence of a ventral pore between 1' and 6" plate (Fig. 2), the cell depicting in Figs. 1a and 2a and that in Figs. 1c and 2b were identified as *Amylax buxus* (Balech) Dodge and *Amylax triacantha* (Jörgensen) Sournia, respectively. These two species seemed to occur 1:1 in the samples, and almost during the same period.

In vivo *fluorescence*

The plastids of both *A. buxus* and *A. triacantha* fluoresced bright orange-fluorescence under the blue-light excitation, which is a characteristic for phycobilin accessory pigment. Every plastid was almost identical in its size and formed U-shape, as shown in Figs. 1b and d. A fluorescence peak at 590 nm in the *in vivo* fluorescent spectrum (Fig. 3) also led the conclusion that these *Amylax* cells possess phycobilin pigment, more specifically phycoerythrin.

Ultrastructure

We succeeded to observe both three cells of *Amylax buxus* (Fig. 4a) and one cell of *A. triacantha* (Fig. 4b) under TEM, and confirmed that ultrastructural features, mostly on that of the endosymbiotic cryptophyte, are comparable among the species. Therefore the descriptions in below will be concerned to *A. buxus* because the sections of this species are much worthy of particular account.

Fig. 4a depicts a longitudinal section of *A. buxus*, and showing a typical

apical horn in this genus. A large dinokaryon located to the posterior half of the cell. In this section, somewhat elongated plastids were locating under the dinokaryon, and U-shaped plastids with a large pyrenoid were in the anterior part. The plastids were abundant, as also shown in the fluorescent micrographs in Figs. 1.

The plastid had a large pyrenoid (Figs. 5a and b; Py) with a stalk connecting the plastid (white arrows) and without any thylakoid intrusion. The pyrenoid had thick starch covering (Figs. 5a and b). The thylakoid had a loose arrangement of three stacks (Fig. 5c), occasionally in two. No girdle lamella was observed. These ultrastructural features in the plastid and the pyrenoid all coincide to that of cryptophyte *Teleaulax* Hill (Clay *et al.*, 1999). Some granules of plastoglobuli were observed in the stroma region (Fig. 5c; PG). The area where the plastid locates was somewhat delimited from the dinoflagellate cytoplasm by surrounding space, but not by obvious membrane (Fig. 5a and b; black arrows). In a close-up of the periplastidal area, a nucleomorph containing electron-dense granules and surrounded by double membranes was observed at the periplastidal area (Figs. 5d and e; NM), where compartmentalized between the double plastid-membranes (PM) and the double plastid endoplasmic reticulum (PER). The PER reached and surrounded the circler space (Figs. 5a,b and d, but much obvious in d; asterisks), thus the space was seemed to be the area where the cryptophyte nucleus had been locating, but digested. Not obvious but the particles of ribosome seemed to attach on the outer surface of PER (Fig. 5e). At some marginal areas of the dinoflagellate, where the plastid is adjacent, there were fragmented membrane profiles in which assignment of the each membranes are not feasible (Fig. 6a; black arrowheads).

In the outer space of the periplastidal area, namely the cryptophycean cytoplasm, the mitochondria with plate-like cristae were observed (Fig. 6b; Cr-M): the feature is typical of the cryptophyte and clearly distinguished from that of dinoflagellate, having the tubular cristae (Fig. 6b; Di-M). Note in this section that there must be boundary membranes between these mitochondria of the different origin, though, the cytoplasm of the cryptophyte and the dinoflagellate were somewhat delimitated by a clearance, not by obvious membrane (Fig. 6b). On the contrary, in the section of Fig. 6c, seven membranes were seen at the boundary of the dinoflagellate and cryptophyte cytoplasm. In the latter case, two sets of lower and upper membranes should be assigned to double plastidal membranes and those of dinoflagellate mitochondrion respectively (white arrows), therefore the inner triple membranes (white arrowheads) include double plastidal ER plus single cryptophyte plasma membrane or dinoflagellate's food vacuolic membrane.

Most of all the cryptophyte remnants had no nuclei as described previously, however, in observing serial sections of a cell, an intact nucleus of cryptophyte cell was observed (Fig. 7a). As far as judging from the serial sections from the single dinoflagellate cell, cryptophyte having the nucleus was solitary among the 14 cryptophyte "remnants". In Fig. 7b, the cryptophyte cell being under the plastidal division process was observed, although not known whether the division was occurred prior to acquiring or after. A cryptophyte remnant seemingly under the whole-digestion was observed (Fig. 7c), but only in a single case.

In any observed sections, typical components of the peduncle, in which the microtubular strands or the microtubular basket, which forms and supports

the feeding tube during ingestion (Schnepf *et al.,* 1985), were not observed.

Phylogenetic analyses

Both *Amylax* species tested in this study (*A. buxus* and *A. triacantha*) have completely identical sequences of nuclear SSU rRNA gene. It is uncertain whether these two species are conspecific or not at present, and the analyses using more rapidly evolving genetic markers (e.g. internal transcribed spacers of ribosomal RNA gene) should be performed in the future. In the ML tree (Fig. 8), the genus *Amylax* is robustly clustered with *Lingulodinium polyedrum* (Stein) Dodge and *A. diacanta* (now regarded as a synonym of *Gonyaulax verior* Sournia) (94% bootstrap probability and 1.00 posterior probability). In addition, this monophyletic lineage was affiliated with other gonyaulacalean species including the non-photosynthetic dinoflagellate *Crypthecodinium cohnii* Seligo although not supported by bootstrap probability.

Twelve clones of plastid SSU rRNA gene for each *Amylax* species were sequenced, and all sequences were completely identical, indicating that the host dinoflagellates engulfed a specific eukaryotic alga as endosymbionts. As shown in the ML tree based on plastid SSU rRNA gene (Fig. 9), the sequences of *A. buxus* and *A. triacantha* are identical to those of photosynthetic species of the dinoflagellate genus *Dinophysis* Ehrenberg and that of one cryptophyte species, *Teleaulax amphioxeia*, which is now recognized as source organisms of *Dinophysis* plastid (Takishita *et al*., 2002, Minnhagen & Janson, 2006, Koike *et al*., 2007). Therefore it is obvious that the plastids of these *Amylax* species are also derived from *T. amphioxeia*.

DISCUSSION

Bralewska & Witek (1995) primarily noted “brilliant yellow-orange to pale red granules were observed in *Gonylaulax triacantha* (=*Amylax triacantha*)”, and the origin of this peculiar plastid is now achieved in our study. This is the first finding of cryptophyte kleptoplastids in the gonyaulacalean dinoflagellate lineage. We did not estimate their photosynthesis, but with regard of the bright *in vivo* fluorescence from the plastids, and the rigid structure of the thylakoid, it is most likely that *A. buxus* and *A. triacantha* are active in photosynthesis and the activity solely support their growth, since heterotrophy in strict sense is not a choice with absence of any food vacuoles.

These *Amylax* species possess plastids identical to those of the photosynthetic species of *Dinophysis*, and the plastids of all these organisms are derived from a cryptophyte species, *Teleaulax amphioxeia*, although not known why always this cryptophyte is the case. Yet, *Amylax* assimilate whole cryptophyte cell while *Dinophysis* retain only cryptophyte plastid. Although incorporation mechanism of plastid in *Dinophysis* species is still in debate, it is plausible that *Dinophysis* get the plastid through feeding a *Teleaulax*-fed ciliate *Myrionecta rubra* (Lohmann) Jankowski (Park *et al.*, 2006). Comparing to this possible indirect incorporation of the plastid, *Amylax* spp. would directly engulf the cryptophyte cell therefore they contained cryptophyte plastid complexes and mitochondria. This was reasonably depicted in patterns of field occurrence of both *Amylax* and *Dinophysis*: since we intended to predict *Dinophysis* bloom by monitoring the *Teleaulax* occurrence in field and conducted enumeration by using *in situ* hybridization with *Teleaulax* plastid SSU rRNA-specific probe (Takahashi *et al.*, 2005, Koike *et al.*, 2007), and found that, on May 30 2006

when the notable *Teleaulax* occurrence peak was detected, maximum occurrence of *Amylax* spp. were also observed while that of *Dinophysis* (*D. fortii)* was on the two weeks later (data not shown). This time-lag seem to be correlated with their differences in the incorporation mechanism: indirect in *Dinophysis* spp. or direct in *Amylax* spp. However, we did not find any peduncle (feeding tube) nor the component of peduncle (microtubule strands or bundles) in the cell sections, therefore the mechanism of engulfing the *Teleaulax* cell in *Amylax* is still not known.

Comparing to the previous finding of cryptophyte endosymbionts in dinoflagellates, the *Amylax* cases are characterized. *Amp. latum* (Horiguchi & Piennar, 1992) and *Amp. poecilochroum* (Lasen, 1988) represented possible primitive stage which may lead to subsequent establishment of a stable symbiotic relationship: *Amp. latum* could take up multiple species of cryptophyte and both *Amp. latum* and *Amp. poecilochroum* delimited cryptophyte cytoplasm by a single phagocytotic membrane. Because the incorporated cryptophytes lost surface structures of the cell (e.g. periplast, flagellar apparatus, ejectsomes) or the plasma membrane itself, they would be taken up myzocytotically, or phagocytotically while digesting surface structure during the incorporation process. In these cases, cryptophyte plastid was surrounded by total five membranes (2 plastidal membranes + 2 plastidal ER + 1 phagocytotic membrane) and the cells were nucleated. On further stage for the endosymbiont process, a fresh water dinoflagellate *G. aeruginosum* (= *G. acidotum or Amp. acidotum ?*) is noted. While *G. aeruginosum* initially retained incorporated cryptophyte (Schnepf *et al*., 1989) as in the same manner of *Amp. latum* (Horiguchi & Piennar, 1992) and *Amp. poecilochroum* (Lasen, 1988)(i.e.

surrounded by a single phagocytotic membrane, nucleated but lacking periplast), it seemed to undergo digestion of cryptophyte nuclei and nucleomorph selectively . In the case of *Amylax* spp., although the mechanisms are not yet clear, they are possible to engulf the cryptophyte through the same mechanisms of former three dinoflagellates because the cryptophytes in the dinoflagellate cytoplasm also apparently lacked components of cell surface. Similarly, the scene depicted in Fig. 6C may show the five membranous boundary (plus two mitochondrial membranes = total seven membranes) surrounding cryptophyte plastid, indicating, at most in the initial stage in the incorporation process, the cryptophyte should be surrounded by a single phagocytotic membrane. But this membrane will be undergone digestion process later, and then formed boundary space, as seen in Figs. 4a and b. Therefore in the light of membrane property, the case of *Amylax* spp. would intermediate the primitive stage (e.g. five membranous boundary of *Amp. latum*, *Amp. poecilochroum*, and *G. aeruginosum*) and the possibly more developed stage of three-membrane bounded cryptophyte plastid as found in *Amphidinium wigrense* Woloszynska

Most intriguingly, the present observation gives evidence that dinoflagellate will digest symbiont nuclei “firstly”. This is already mentioned in *G. aeruginosum and Pfiesteria piscicida* (Lewitus *et al.*, 1999), and now in the case of *Amylax,* it is observed that the nucleus content is digested while the nucleus membranes are retained. This process is fairly unbelievable and the mechanism is far unknown. Even if the genes for plastid-targeted proteins are retained in the cryptophyte nucleomorph genome, they are limited up to 30 genes (Douglas *et al.*, 2001, Lane *et al.*, 2007), and nucleus-encoded genes are essential to maintain plastid function. In the case of a cryptophyte plastid robbing ciliate

Myrionecta rubra (Lohmann) Jankowski, most of the phagocytosed cryptophyte are also anucleated, but small number of the retained cryptophyte nucleus, being compelled to express photosynthetic genes, serve multiple cryptophyte plastids (Johnson *et al*., 2007). This may be also the case in *Amylax* in which the one intact nucleus of cryptophyte endosymbiont (Fig. 7a) serves multiple anucleated cryptophyte endosymbionts. Otherwise, since no SSU rRNA gene sequence possibly originated from cryptophyte nucleus was detected in our PCR-based survey in which 12 clones of nuclear SSU rRNA gene were randomly sequenced, finding of a endosymbiont nucleus under the serial-sectioning might be incidental, viz. rather just being not-yet-digested one. If eliminating any possibilities of the nucleus contribution, the plastids in the *Amylax* cell should be nondurable in life and photosynthesis, as the cases of other kleptoplastidic species; 1-2 days retention in *G. gracilentum* (Skovgaard, 1998), and up to 14 days in *G. aeruginosum* (Fields and Rhodes, 1991). Not only concern to the case of *Amylax*, but we further need to inquire how the photosynthesis is controlled in many of kleptoplastidic species, to know whether these kleptoplastidic cases are actually clever at accomplishing to fully established (genetically integrated) plastid in evolution, or just the opportunistic behavior to get easy-energy.

ACKNOWLEDGEMENT

The authors express their sincere thanks to Mrs. Kanae Koike for assisting and accomplishing with the TEM observations. This work was supported by a Grand-in-Aid (No. 17380125) for Scientific Research from the Ministry of Education, Culture, Sports, Science and Technology of Japan to K. K.

References

Bralewska, J. M. and Witek, Z. 1995. Heterotrophic dinoflagellates in the ecosystem of the Gulf of Gdansk. *Mar. Ecol. Prog. Ser.* **117**:241-48.

Clay, B. L., Kugrens, P. and Lee, R. E. 1999. A revised classification of Cryptophyta. *Bot. J. Linean Soc.* **131**:131-51.

Douglas, S., Zauner, S., Fraunholz, M., Beaton, M., Penny, S., Deng, L. T., Wu, X. N., Reith, M., Cavalier-Smith, T. and Maier, U. G. 2001. The highly reduced genome of an enslaved algal nucleus. *Nature* **410**:1091-96.

Eriksen N. T., Hayes K. C., and Lewitus, A. 2002. Growth responses of the mixotrophic dinoflagellates, *Cryptoperidiniopsis* sp. and *Pfiesteria piscicida*, to light under prey-saturated conditions. *Harmful Algae* **1**:191-203.

Fritz, L. and Triemer, R. E. 1985. A rapid, simple technique utilizing calcofluor white M2R for the visualization of dinoflagellate thecal plates. *J. Phycol.* **21**:662-64.

Gast, R. J., Moran, D. M., Dennett, M. R. and Caron, D. A. 2007. Kleptoplasty in an Antarctic dinoflagellate: caught in evolutionary transition? *Environ. Microbiol.* **9**:39-45.

Guindon, S. and Gascuel, O. 2003. A simple, fast, and accurate algorithm to estimate large phylogenies by maximum likelihood. *Systematic Biology* **52**:696-704.

Horiguchi, T. and Piennar, R. N. 1992. *Amphidinium latum* (Dinophyceae), a sand-dwelling dinoflagellate feeding on cryptomonads. *Jpn. J. Phycol.* **40**:353-63.

Jakobsen, H. H., Hansen, P. J. and Lasen, J. 2000. Growth and grazing responses of two chloroplast-retaining dinoflagellates: effect of irradiance and prey species. *Mar. Ecol. Prog. Ser*. **201**:121-128.

Johnson, M. D., Oldach, D., Delwiche, C. F. and Stoecker, D. K. 2007. Retention of transcriptionally active cryptophyte nuclei by the ciliate *Myrionecta rubra*. *Nature* **445**:426-28.

Koike, K., Nishiyama, A., Takishita, K., Kobiyama, A. and Ogata, T. 2007. Appearance of *Dinophysis fortii* following blooms of certain cryptophyte species. *Mar. Ecol. Prog. Ser.* **337**:303-09.

Koike, K., Sekiguchi, H., Kobiyama, A., Takishita, K., Kawachi, M., Koike, K. and Ogata, T. 2005. A novel type of kleptoplastidy in *Dinophysis* (Dinophyceae): Presence of haptophyte-type plastid in *Dinophysis mitra*. *Protist* **156**:225-37.

Lane, C. E., van den Heuvel, K., Kozera, C., Curtis, B. A., Parsons, B. J., Bowman, S. and Archibald, J. M. 2007. Nucleomorph genome of *Hemiselmis andersenii* reveals complete intron loss and compaction as a driver of protein structure and function. *Proc. Natl. Acad. Sci. USA* **104:**19908-19913.

Lasen, J. 1988. An ultrastructural study of *Amphidinium poecilochroum* (Dinophyceae), a phagotrophic dinoflagellate feeding on small species of cryptophytes. *Phycologia*

27:366-77.

Lewitus, A. J., Glasgow, H. B. Jr. and Burkholder J. M. 1999. Kleptoplastidy in the toxic dinoflagellate *Pfiesteria piscicida* (Dinophyceae). *J. Phycol.* **35**:303-312.

Lopez-Garcia, P., Philippe, H., Gail, F. and Moreira, D. 2003. Autochthonous eukaryotic diversity in hydrothermal sediment and experimental microcolonizers at the Mid-Atlantic Ridge. *Proc. Natl. Acad. Sci. USA* **100**:697-702.

Minnhagen, S. and Janson, S. 2006. Genetic analyses of *Dinophysis* spp. support kleptoplastidy. *FEMS Microbiol. Ecol.* **57**:47-54.

Park, M. G., Kim, S., Kim, H. S., Myung, G., Kang, Y. G. and Yih, W. 2006. First successful culture of the marine dinoflagellate *Dinophysis acuminata*. *Aquat. Microbial Ecol.* **45**:101-06.

Rodríguez, F., Oliver, J. L., Marín, A. and Medina, J. R. 1990. The general stochastic model of nucleotide substitution. *J. Theor. Biol.* **142**:485-501.

Ronquist, F. and Huelsenbeck, J. P. 2003. MrBayes 3: Bayesian phylogenetic inference under mixed models. *Bioinformatics* **19**:1572-74.

Saldarriaga, J. F., Taylor, F., Cavalier-Smith, T., Menden-Deuer, S. and Keeling, P. J. 2004. Molecular data and the evolutionary history of dinoflagellates. *Eur. J. Protistol.* **40**:85-111.

Schnepf, E., Winter, S. and Mollenhauer, D. 1989. *Gymnodinium aeruginosum* (Dinophyta): a blue-green dinoflagellate with a vestigial anucleate, cryptophycean endosymbiont. *Plant Syst. Evol.* **164**:75-91.

Skovgaard, A. 1998. Role of chloroplast retention in a marine dinoflagellate. *Aquat. Microb. Ecol.* **15**:293-301.

Takahashi, Y., Takishita, K., Koike, K., Maruyama, T., Nakayama, T., Kobiyama, A. and Ogata, T. 2005. Development of molecular probes for *Dinophysis* (Dinophyceae) plastid: A tool to predict blooming and explore plastid origin. *Mar. Biotechnol.* **7**:95-103.

Takishita, K., Koike, K., Maruyama, T. and Ogata, T. 2002. Molecular evidence for plastid robbery (Kleptoplastidy) in *Dinophysis*, a dinoflagellate causing diarrhetic shellfish poisoning. *Protist* **153**:293-302.

Takishita, K., Nakano, K. and Uchida, A. 1999. Preliminary phylogenetic analysis of plastid-encoded genes from an anomalously pigmented dinoflagellate *Gymnodinium mikimotoi* (Gymnodiniales, Dinophyta). *Phycol. Res.* **47**:257-62.

Thompson, J. D., Higgins, D. G. and Gibson, T. J. 1994. Clustal-W - improving the sensitivity of progressive multiple sequence alignment through sequence weighting, position-specific gap penalties and weight matrix choice. *Nucleic Acids Res.* **22**:4673-80.

Wilcox, L. W. and Wedemayer, G. J. 1985. Dinoflagellate with blue-green chloroplasts derived from an endosymbiotic eukaryote. *Science* **227**:192-94.

Figure legends

Fig.1. Light (left column) and epifluorescent (right column) micrographs of *Amylax buxus* (a and b) and *Amylax triacantha* (c and d).

Fig. 2. Epifluorescent micrographs (under UV excitation) of *Amylax buxus* (a) and *Amylax triacantha* (b), stained with a cellulose strainer calcofluor-white M2R. Note that obscure but apparent discontinuity between the thecal plates of 1' and 6" can be recognized in (b) but not in (a), indicating a cell shown in (b) possess a ventral pore, which is a criterion of *A. triacantha* from *A. buxus*.

Fig. 3. An *in vivo* fluorescence spectrum of a *Amylax buxus* cell, under blue-light excitation (emission 460 to 490 nm, barrier 515 nm), showing emission peak at 581 nm (an arrow).

Fig. 4. Transmission electron micrographs of longitudinal sections of *Amylax buxus* (a) and *A. triacantha* (b). Cryptophyte cells, with a U-shaped plastid and a large pyrenoid, are observed in the marginal region of the cells (arrows). DK, dinokaryon.

Fig. 5. Close-up of the cryptophyte cells in *Amylax buxus*. The cells (a, b) are seemingly delimitated from the dinoflagellate cytoplasm by the surrounding thin space (black arrows). They have a large prominent pyrenoid (Py) with a stalk (an white arrow). Note that they have no nuclei, but instead, have circler space (asterisks). The plastid has thylakoids arranged in loose stacks of three (c), occasionally of two. In close up at the plastid region (d, e), a double-membrane

bound nucleomorph (NM) with electron-dense granules, is observed. It locates within the space between the plastid double- membranes (PM) and the further over-layered double- plastidal endoplasmic reticulum (PER). The reticulum seemingly leads to the outer-most membranes of the circular space (asterisks).

Fig. 6. Close-up of the region between the cryptophyte cell and the dinoflagellate cytoplasm. At marginal areas of the dinoflagellate, where the plastid (Pl) is adjacent, there were fragmented membrane profiles in which assignment of the each membranes are not feasible (a; black arrowheads). In the cryptophycean cytoplasm (b), the mitochondria with plate-like cristae were observed (Cr-M): the feature is typical of the cryptophyte and clearly distinguished from those of dinoflagellate, having the tubular cristae (Di-M). In the section of (c), seven membranes (white arrowheads and arrows) were seen at the boundary of the dinoflagellate (where Di-M locating) and cryptophyte cytoplasm (where Cr-M locating). Two sets of lower and upper membranes should be assigned to double plastidal membranes and those of dinoflagellate mitochondrion respectively (the white arrows), therefore the inner triple membranes (the white arrowheads) include double plastidal ER plus single cryptophyte plasma membrane or dinoflagellate's food vacuolic membrane.

Fig. 7. Various types of cryptophytes in a *Amylax buxus* cell. There can be seen a cryptophyte cell with intact nucleus (a; Cr-N) among 14 anucleated cryptophytes. In another, a cryptophyte cell being under the plastidal division process is observed (b), meanwhile a cryptophyte remnant seemingly under whole-digestion (c).

Fig. 8. Maximum likelihood phylogeny of nuclear SSU rRNA gene from dinoflagellates. Two species of apicomplexans were used to root the tree. Bootstrap probabilities are shown for nodes with support over 50%. The thick branches represent branches with over 0.90 Bayesian posterior probabilities.

Fig. 9. Maximum likelihood phylogeny of plastid SSU rRNA gene from cryptophytes and dinoflagellates with cryptophyte-derived kleptoplastids. Two species of red algae were used to root the tree. Bootstrap probabilities are shown for nodes with support over 50%. The thick branches represent branches with over 0.90 Bayesian posterior probabilities

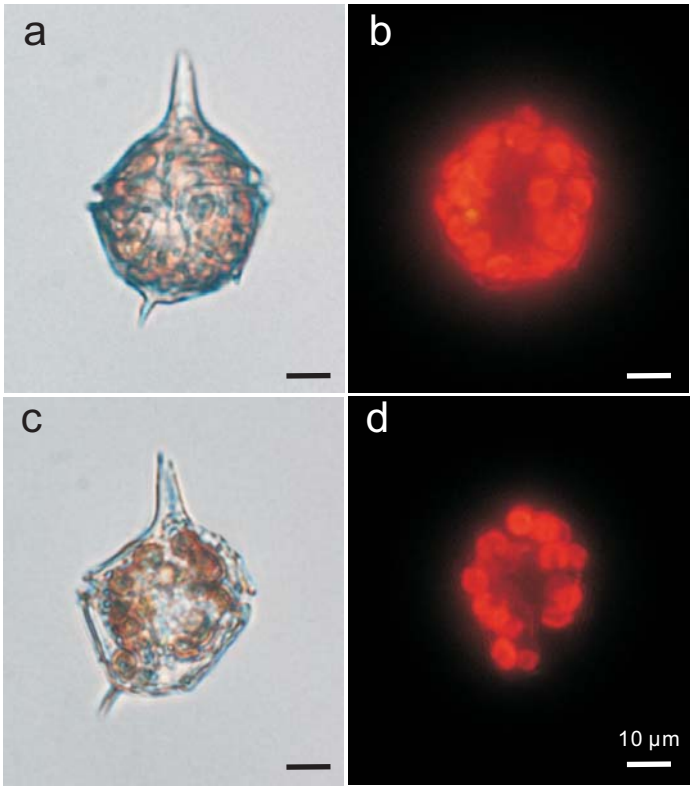
a
b
c
d
10 µm

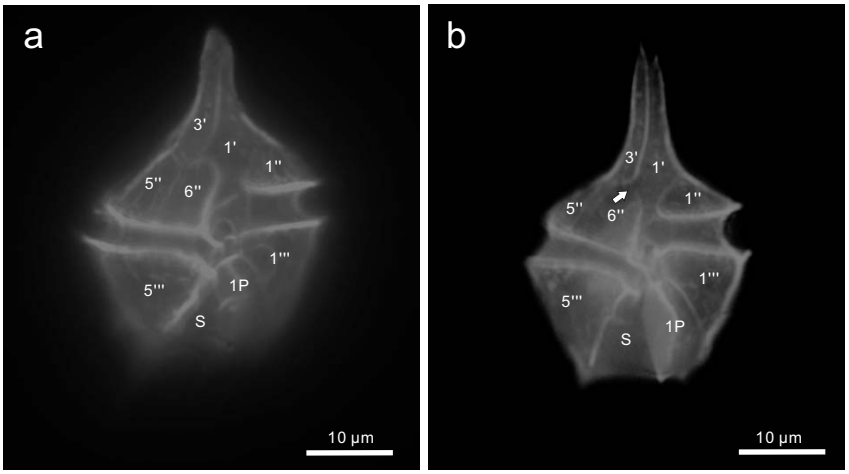
a
3'
1'
1''
5''
6''
1'''
5'''
1P
S
10 µm
b
3'
1'
5''
6''
1''
1'''
5'''
S
1P
10 µm

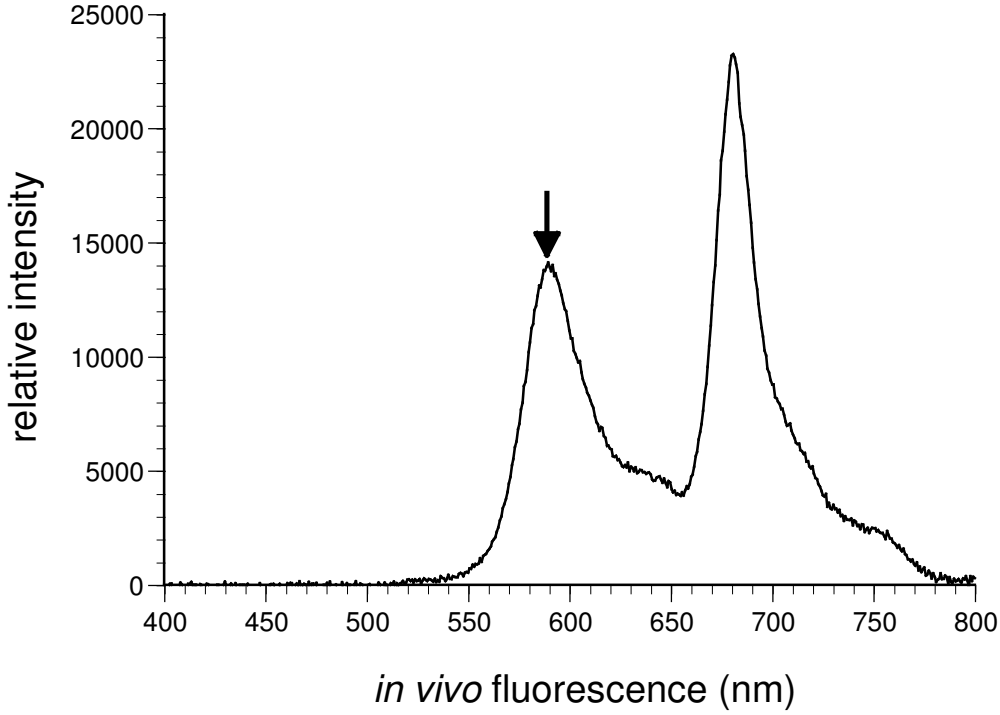
25000
20000
15000
10000
5000
0
relative intensity
400
450
500
550
600
650
700
750
800
in vivo fluorescence (nm)

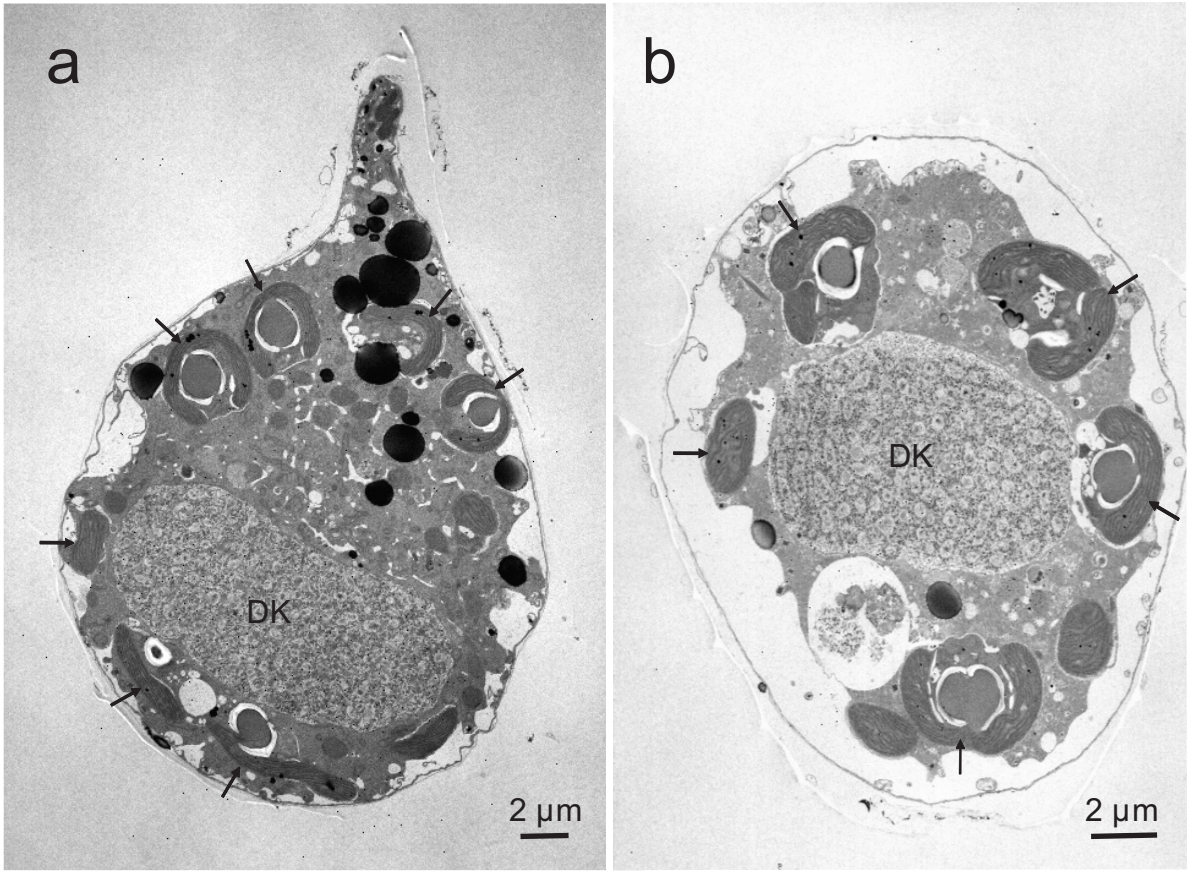

Fig. 4. Koike & Takishita

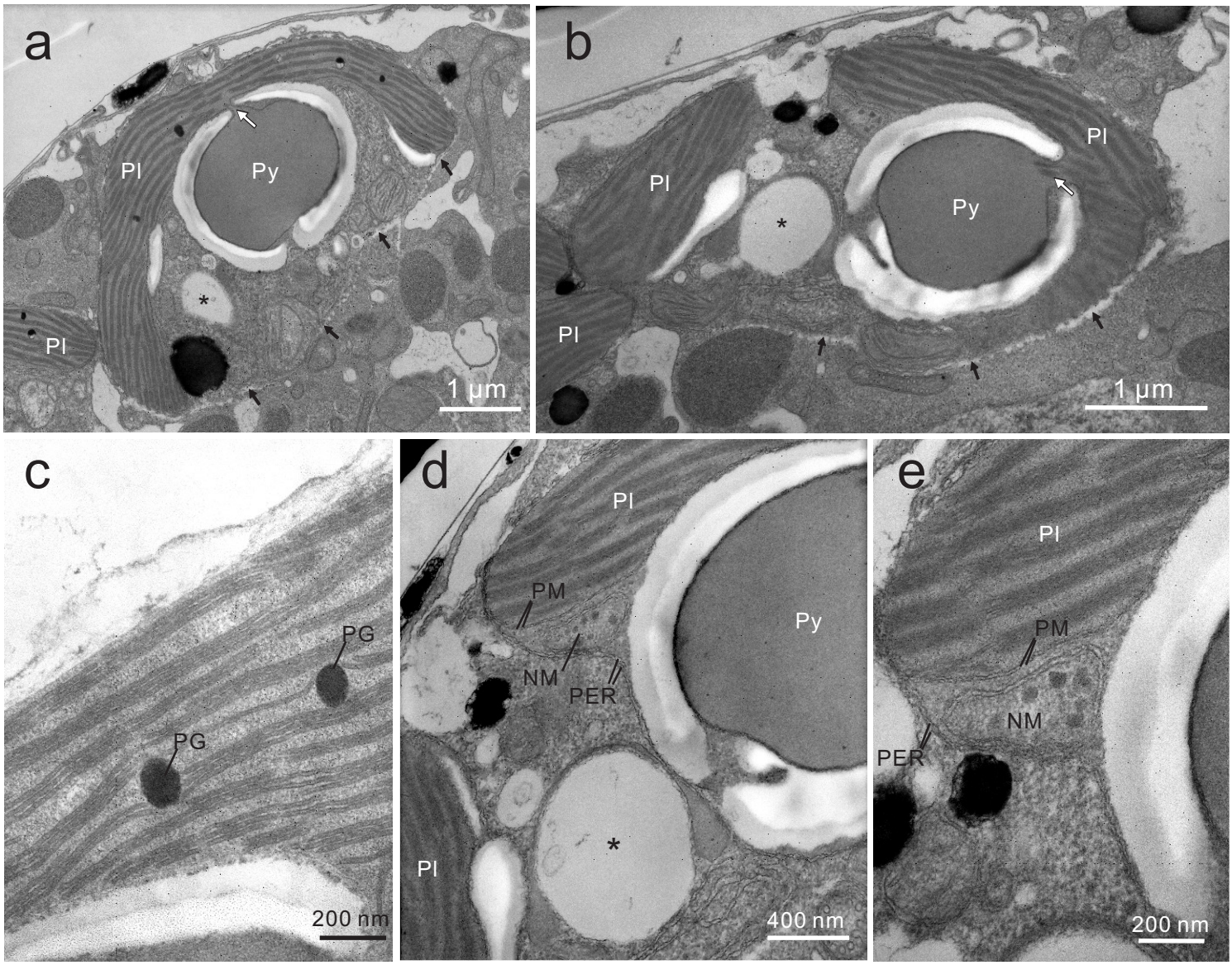

Fig. 5. Koike & Takishita

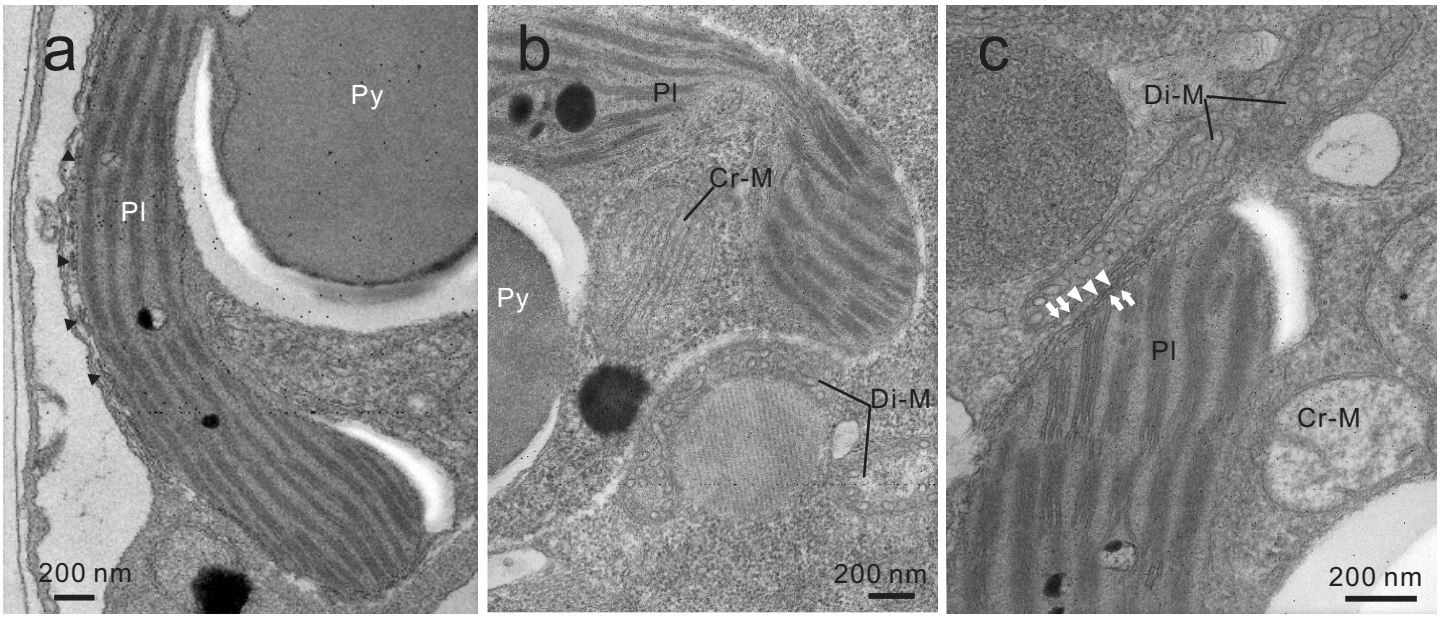

Fig. 6. Koike & Takishita

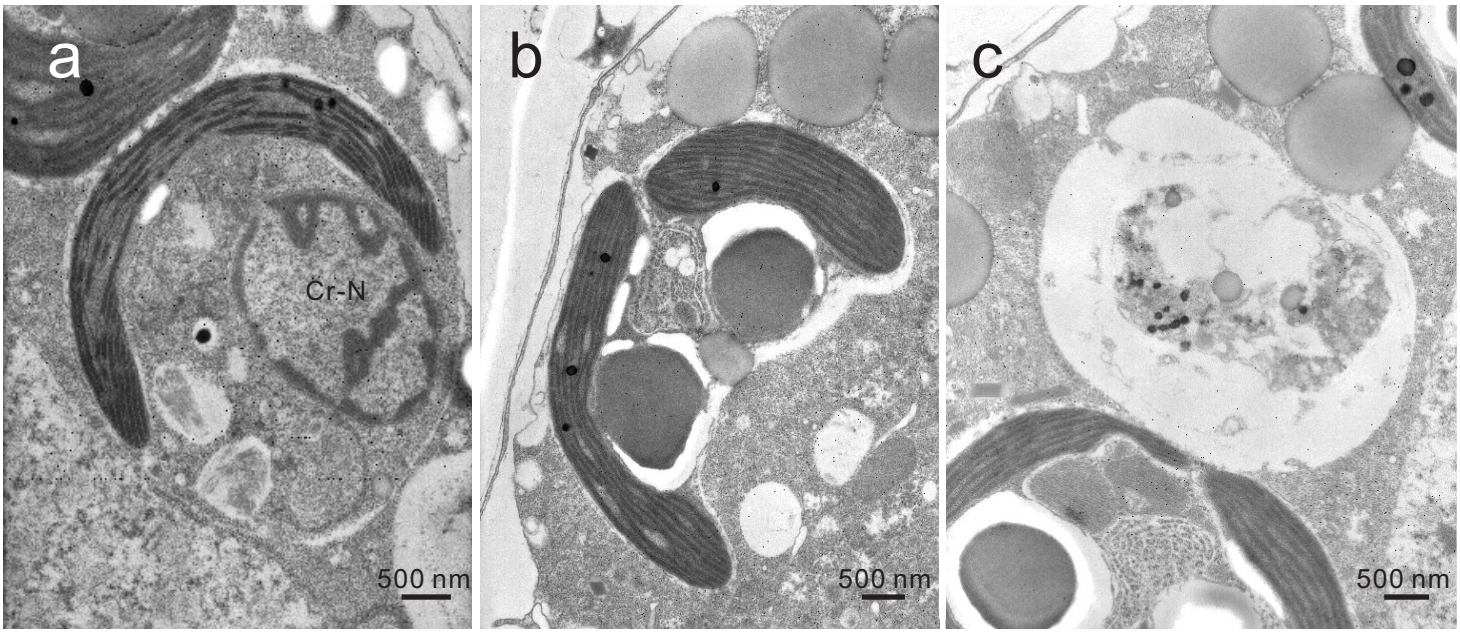

Fig. 7. Koike & Takishita

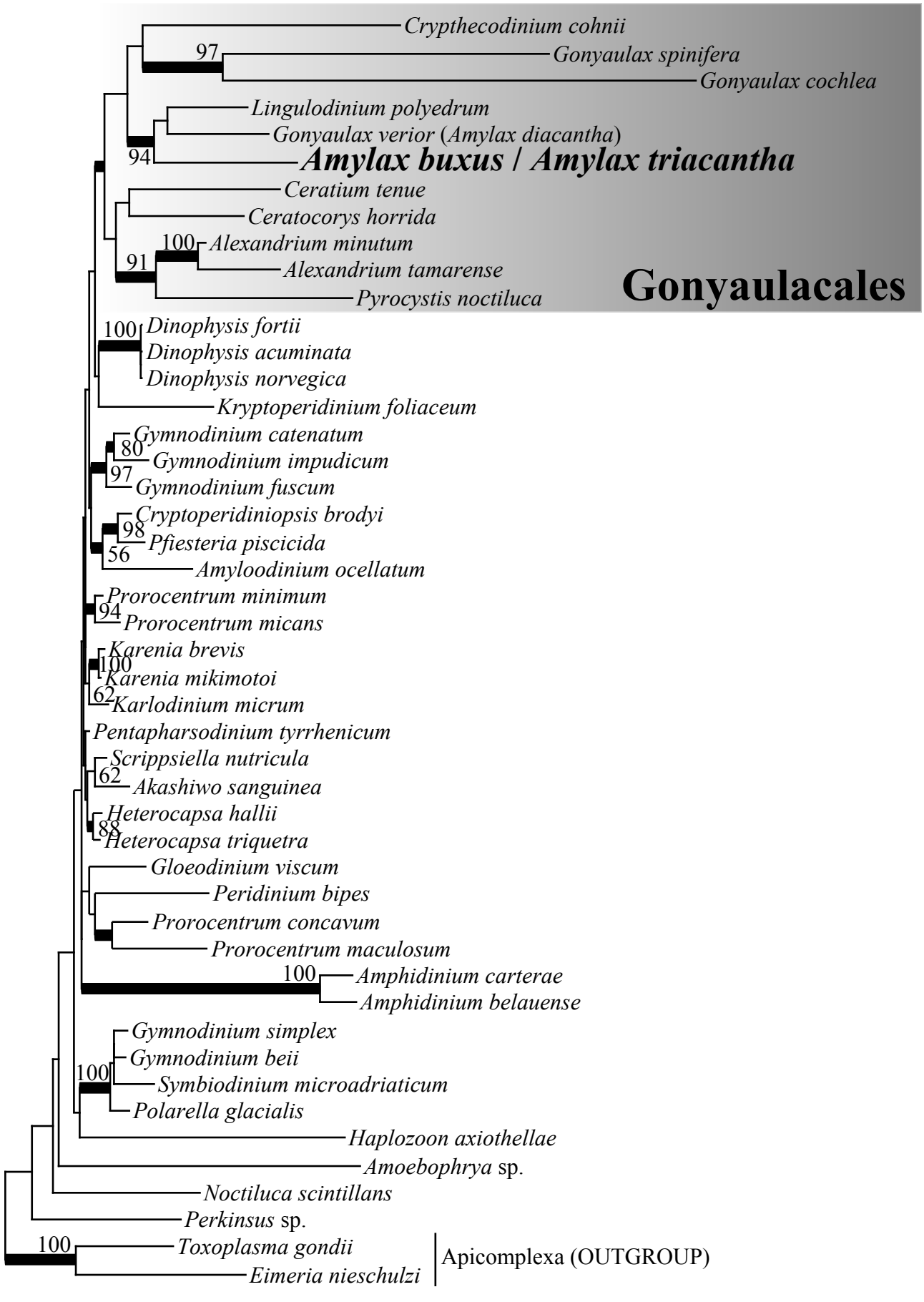
Crypthecodinium cohnii
97
Gonyaulax spinifera
Gonyaulax cochlea
Lingulodinium polyedrum
Gonyaulax verior (Amylax diacantha)
94
Amylax buxus / Amylax triacantha
Ceratium tenue
Ceratocorys horrida
100
Alexandrium minutum
91
Alexandrium tamarense
Pyrocystis noctiluca
Gonyaulacales
100
Dinophysis fortii
Dinophysis acuminata
Dinophysis norvegica
Kryptoperidinium foliaceum
Gymnodinium catenatum
80
Gymnodinium impudicum
97
Gymnodinium fuscum
Cryptoperidiniopsis brodyi
98
Pfiesteria piscicida
56
Amyloodinium ocellatum
Prorocentrum minimum
94
Prorocentrum micans
Karenia brevis
100
Karenia mikimotoi
62
Karlodinium micrum
Pentapharsodinium tyrrhenicum
Scrippsiella nutricula
62
Akashiwo sanguinea
Heterocapsa hallii
88
Heterocapsa triquetra
Gloeodinium viscum
Peridinium bipes
Prorocentrum concavum
Prorocentrum maculosum
100
Amphidinium carterae
Amphidinium belauense
Gymnodinium simplex
Gymnodinium beii
100
Symbiodinium microadriaticum
Polarella glacialis
Haplozoon axiothellae
Amoebophrya sp.
Noctiluca scintillans
Perkinsus sp.
100
Toxoplasma gondii
Eimeria nieschulzi
Apicomplexa (OUTGROUP)
0.05 substitution/site

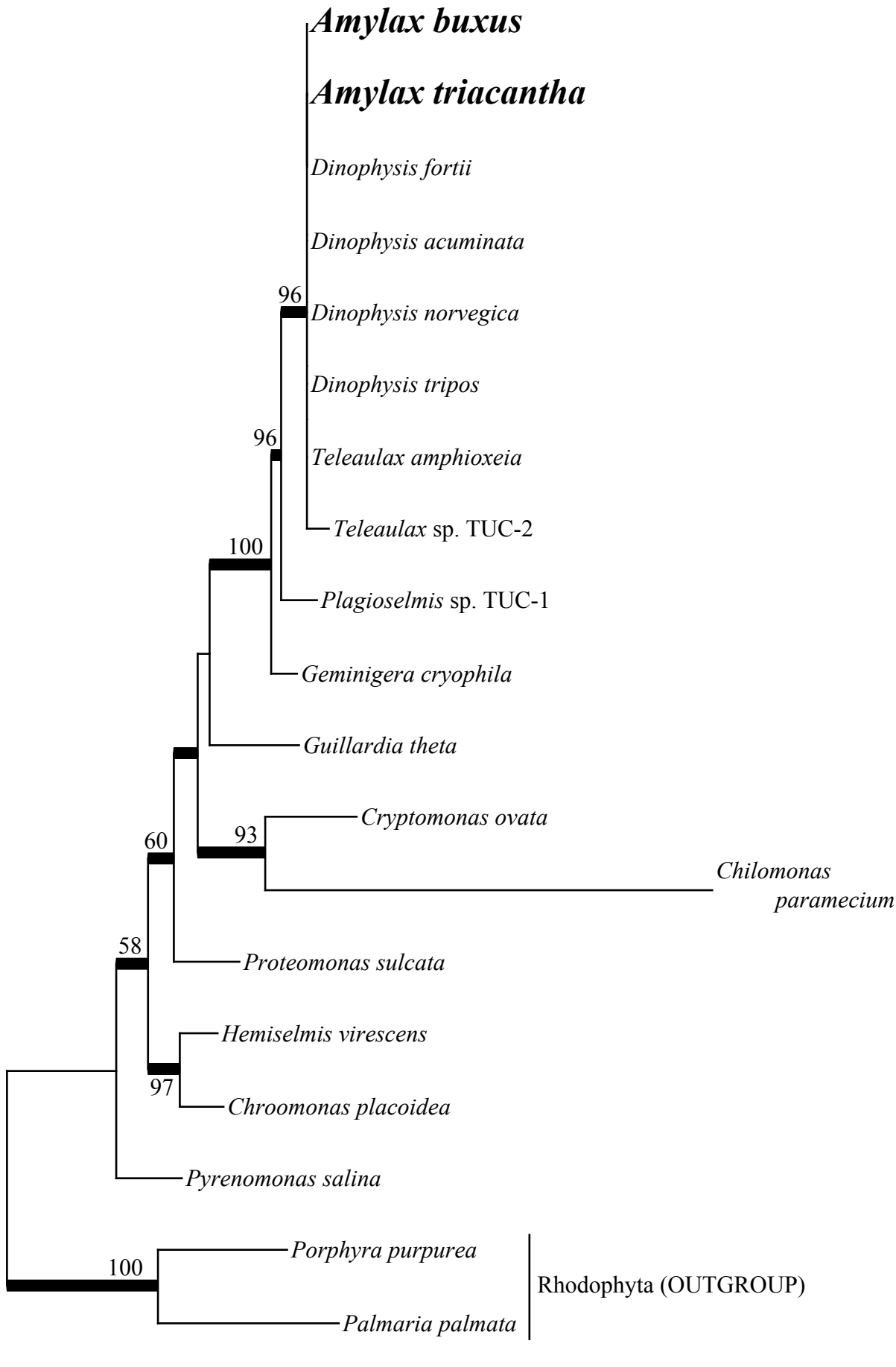
Amylax buxus
Amylax triacantha
Dinophysis fortii
Dinophysis acuminata
96
Dinophysis norvegica
Dinophysis tripos
96
Teleaulax amphioxeia
Teleaulax sp. TUC-2
100
Plagioselmis sp. TUC-1
Geminigera cryophila
Guillardia theta
Cryptomonas ovata
60
93
Chilomonas paramecium
58
Proteomonas sulcata
Hemiselmis virescens
97
Chroomonas placoidea
Pyrenomonas salina
Porphyra purpurea
100
Palmaria palmata
Rhodophyta (OUTGROUP)
0.02 substitution/site